CHEMICAL ENGINEERING TRANSACTIONS
VOL. 114, 2024
A publication of AIDIC
The Italian Association of Chemical Engineering
Online at www.cetjournal.it
Guest Editors: Petar S. Varbanov, Min Zeng, Yee Van Fan, Xuechao Wang

ISBN 979-12-81206-12-0; **ISSN** 2283-9216
DOI: 10.3303/CET24114007

Analysis of Environmental Variables during Apple Dehydration

Guillermo Martínez-Rodríguez[a,*], Rosa A. Olmos-Cruz[a], Evangelina Sánchez-García[b], Juan-Carlos Baltazar[c]

[a]Department of Chemical Engineering, University of Guanajuato, Guanajuato 36050, Mexico
[b]Department of Pharmacy, University of Guanajuato, Guanajuato 36050, Mexico
[c]Texas A&M Engineering Experiment Station (TEES), Texas A&M University, College Station 3581, U.S.A.
guimarod@ugto.mx

Variability of the solar resource represents a challenge in the solar dehydration of fruits. To control the kinetics of solar dehydration, the behavior of the variables with the greatest impact on fruit dehydration is characterized: ambient temperature, relative humidity, wind speed and irradiance. 876,000 data of these four environmental variables were obtained from a meteorological station located in the city of Guanajuato (Mexico). The data correspond to the dehydration period of 8:00 to 18:00 h during the year 2023. Classified into quartiles and represented in Box-Whiskers diagrams, the data was analyzed in their distribution and symmetry. Experimental tests were carried out for apple dehydration during the four seasons of the year 2023, considering the shrinkage of the fruit (radius and thickness). The impact of environmental variables on the drying kinetics was determined. The shortest drying times of up to 5 h (April), were obtained even when the highest levels of wind speed were recorded (6.65 m/s). Ambient temperature and relative humidity significantly impact drying kinetics, increasing drying times by up to 40 %. This analysis allows standardizing the dehydration process in an indirect solar dehydrator even under variable punctual, monthly and seasonal environmental conditions.

1. Introduction

Solar dehydration is a conservation process widely used to extend the shelf life of foods and is characterized by generating high quality products with high added value, in addition to being an alternative used to reduce costs (Kamarulzaman et al., 2021). Already from 1983 to 1987, the scientific community gathered in Europe, which can be referred to the first version of the book (Jowitt et al., 1983) and the second version (Jowitt et al., 1987), had integrated important conclusions regarding the fact that the type of material in the food and the type of processing it receives impact its physicochemical properties.

The intermittent nature of solar energy is one of the main factors impacting solar dehydration. Intermittency is related to atmospheric variables such as irradiance level, ambient temperature, relative humidity and wind velocity that can compromise the fruit dehydration process. Determining the amount and flow of energy that interacts indirectly or directly with the food is one of the best alternatives compared to traditional open air drying that is limited by climate dependence (Aviara et al., 2014). Meteorological conditions have a considerable impact on the operation of the solar device and its variability is conditioned by the geographical location where the dehydration process takes place. In general, the process is affected in regions with high relative humidity, low levels of irradiance and high wind velocities, the latter having an impact on convective losses that are significant when the wind speed is above 2.5 m/s (Duffie and Beckman, 2013). Nukulwar and Tungikar (2020) studied different types of dehydrators for different products that require a specific drying environment, pointing out that solar radiation, relative humidity, and ambient temperature are the main variables that must be considered to design a solar dryer. Benseddik et al. (2018) studied the behavior of irradiance, ambient temperature and relative humidity on a solar dryer through isopleth graphs of 7 cities in Algeria. They determined the variables data distribution using the Kernel method and concluded that for two cities there would be very high yields in summer. Barros-Silva (2022) studied the performance of an indirect solar dehydrator in different climates and

Paper Received: 8 July 2024; Revised: 23 August 2024; Accepted: 24 November 2024
Please cite this article as: Martínez-Rodríguez G., Olmos-Cruz R.A., Sánchez-García E., Baltazar J.-C., 2024, Analysis of Environmental Variables During Apple Dehydration, Chemical Engineering Transactions, 114, 37-42 DOI:10.3303/CET24114007

meteorological conditions for the dehydration of silver banana in Brazil. They concluded high temperature and low relative humidity of the ambient air, impacted on the drying time (11 h in summer vs 16 h in winter). The study of the performance of indirect solar dehydrators under different meteorological conditions has also been used to select the energy storage that can be incorporated (Chaatouf et al., 2023). Majdi and Esfahani (2018) developed a two-dimensional analytical model that describes the simultaneous heat and mass transfer process for apple drying without considering shrinkage; they used a convective dehydrator and the maximum error between the theoretical and experimental results was 1.4 %.
In this work, a statistical analysis was carried out to study the trend and the relationship between four environmental conditions and the impact they have during apple dehydration in the city of Guanajuato over the course of a year. An indirect solar dehydration tower with a loading capacity of 5 kg of fresh product was used, which was operated in a controlled manner at 45 °C during the four seasons of the year to validate the relationships found. Fruit shrinkage was considered, both thickness and radius. The summer drying time of 5 h is less than the 8 h reported in the literature.

2. Methodology

From the review in the open literature, four environmental variables were selected that define the captured energy, the humidity absorption capacity from the air and the heat loss in a drying device, since in turn other important variables such as the overall heat transfer coefficient and the mass transfer coefficient are modified by changing the environmental variables in question. To know the variability of environmental conditions throughout the year, a descriptive statistical technique (Scheff, 2016) such as the Box-whisker diagram or Box-plot was used. These variables were studied to quantify their impact on the kinetics of a solar dehydrator.

2.1 Statistical analysis of environmental variables

876,000 data taken from 8:00 to 18:00 h on ambient temperature, relative humidity, wind velocity and irradiance for 365 days in the year 2023 of the city of Guanajuato (Mexico) were used. They were classified into sets of 600 data per day for each environmental variable (2400 total daily data). The data were sorted in ascending order by day, by month and by year. The median (Q_2) was calculated followed by the quartiles Q_1 and Q_3 Eq(1), as well as the interquartile range ($IQR = Q_3 - Q_1$). With this information, the box of a Box-whiskers or Box-plot diagram was plotted using JMP software. The interquartile range specifies the width of the box and gives information about when any of the values are far from the central value (Figure 1). To plot the 'whiskers', the upper limit (UW), is calculated with [$\mathrm{UW} = Q_3 + 1.5\ (IQR)$], and lower limit (LW) is calculated with [$\mathrm{LW} = Q_1 - 1.5\ (IQR)$]. Data outside these limits are identified as outliers and are displayed as individual points outside the upper and lower limits of the whiskers.

$$Q_k = \frac{a(N+1)}{100} \tag{1}$$

where N is the total data number and a is the percentile value depending on the quartile to be calculated.

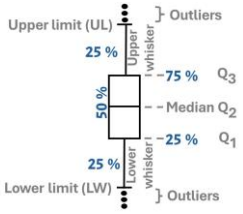

Figure 1: General Box-whiskers or Box-plot diagram.

The Box-plot diagram shows the distribution of the data ordered into four quartiles that contain 25, 50 and 75 % of the data, also known as the 25th, 50th and 75th percentiles (Gutiérrez-Pulido and De-la-Vara, 2013). Quartiles make it easier to analyze the distribution of the data, a wide interquartile range indicates great variability, while a small one indicates less variability. Changes in the boxes allow us to notice trends in data during the year.

2.2 Drying kinetics

The moisture content of the cylindrical apple samples (M) was calculated on a wet basis using Eq(2).

$$M = \frac{m_i - m_s}{m_i}\ x\ 100 \tag{2}$$

where m_i and m_s are the wet basis weight of one thin apple slice, and dry weight respectively. The latter was obtained by drying all the samples in an oven at 105 °C for 24 h. The calculated average initial moisture content of the apple was 86 %.Fick's Second Law of diffusion describes the movement of water molecules within the food and is expressed with Eq(3) which relates the change in moisture content with respect to time, which is equal to the dot product between the vector differential and scalar gradient of moisture content, M.

$$\frac{\partial M}{\partial t} = D\,\nabla \cdot (\nabla M) \tag{3}$$

Left term represents the change in the moisture content of the food (M) over time, while the right side represents molecular diffusion, which describes how the substance spreads in the medium due to the existing moisture gradient, with D being the diffusion coefficient [m^2/s]. To solve Eq(3), it is assumed that (Djebli et al., 2020): a) the distribution of moisture content is uniform throughout the sample, b) external resistances are negligible and c) the process is isothermal. With the premise that moisture is transferred solely by diffusion, with constant temperature and diffusivity coefficients, the analytical solution of Fick's equation for an infinite flat plate is Eq(4) and for an infinite hollow cylinder is Eq(5). These analytical solutions given by Crank (1975) are subject to an initial condition $t = 0$, $M = M_o$, and boundary conditions, $x = 0$, $\frac{\partial M}{\partial x} = 0$, and $x = b$, $M = M_e$. Where λ_j are the roots of the zero-order Bessel function and l is half the thickness. The diffusion coefficient (D) is obtained by multiplying Eq(4) and Eq(5) to obtain the Rani and Tripathy (2021) analytical solution, Eq(6). Where t is the time [s], R and z are the radius and the initial thickness of the sample [m], α_1 is the first root of the zero-order Bessel function and M_r is the moisture removal rate that relates the gradient of the current moisture content at time t, with respect to the maximum gradient that exists in the drying system.

$$M_r = \left(\frac{8}{\pi^2}\right)\sum_{i=0}^{\infty}\frac{1}{(2i+1)^2}\exp\left[-(2i+1)^2\pi^2\frac{D}{l^2}\,t\right] \tag{4}$$

$$M_r = \sum_{j=1}^{\infty}\frac{4}{\lambda_j^2}\exp\left[-\frac{D\lambda_j^2\,t}{R^2}t\right] \tag{5}$$

$$M_r = \frac{32}{\pi^2}\sum_{\mathrm{i}=0}^{\infty}\sum_{j=1}^{\infty}\frac{1}{\alpha_j^2(2i+1)^2}\exp\left[-\frac{D\lambda_j^2\,t}{R^2}\left(\frac{\alpha_j^2}{R^2}+(2i+1)^2\frac{\pi^2}{z^2}\right)t\right] \tag{6}$$

The diffusion coefficient describes the velocity of the drying kinetics, as it dictates the velocity of the process during the decreasing period. At this point the amount of free water on the surface of the material has already been completely evaporated (constant period), which causes the formation of the concentration gradient between the internal and external part of the food, generating the migration of the moisture content from the center to its surface. By solving Fick's second Law, the diffusivity is determined experimentally, which is a function of the drying air velocity, the temperature and relative humidity of the air. In turn, the temperature depends on the irradiance and the absorber area. The solar dehydrator is of the indirect tower type, so the wind speed does not directly impact the mass transfer by diffusion in the apple sample.

2.3 Drying tests

The tests were carried out during the 4 seasons of the year 2023 in the city of Guanajuato, Mexico, in an indirect (tower-shaped) forced convection solar dehydrator. 5 kg green apple (Golden) was used in each test carried out, cut into cylindrical slices with the same thickness and diameter (3 mm thick, 5 to 6 cm in radius) that were dehydrated in 10 trays. Three samples called A, B, and C from each tray were selected to monitor the drying kinetics carried out at 45 °C. A, B and C are equidistant from each other.

3. Results

This section presents the results of the statistical analysis applied to the data recorded throughout the year 2023 of four environmental variables, ambient temperature, relative humidity, wind speed and irradiance. The Box-plot data classification technique was applied, resulting in 18,250 single-variable data grouped monthly.

3.1 Evaluation of environmental variables based on useful heat

Figure 2a shows the monthly parabolic behavior of ambient temperature in the year 2023 and Figure 2b shows the biases or asymmetries of data. The studied period was from 8:00 to 18:00 h, being maximum irradiance 1,227 W/m^2 and minimum 272.6 W/m^2. Table 2 shows values of mean (Q2) and IQR of the four studied variables.

In January, 50 % of the temperatures fluctuated between 16.5 and 20.9 °C (Q1 and Q3), that is, an IQR of 4.4 °C. The bottom half of the January box (the 25 % of the data that is below 19.30°C) is larger than the top half, meaning there is more variation in that data. The total of outlier ambient temperature data was 519 throughout the year, this is 0.23 %, which is not significant. The measures of central tendency, mean and median, do not coincide in the twelve months. In the months of March, April and May, there are ambient temperature values in which the boxes overlap, these range from 25.8 °C (March, Q3) to 21.87 °C (May, Q1), manifesting a constant range of ambient temperature values in those months. In the month of April, a greater variability of the data is seen in the lower half box (Q1 to Q2), which expands the temperature range from 21.3 to 24.3 °C. In June, a very homogeneous distribution of the data can be seen (the halves of the boxes are almost the same size), however, the great data variability between the boxes and the whiskers is evident along their length. The minimum and maximum average values of ambient temperature during June are 16.5 and 35 °C; the temperatures recorded for 50 % of the data inside the box are 24.4 and 30.5 °C (Q1 and Q3), this represents a variability in the monthly temperature of 6.1 °C (IQR), the highest variability of the year.

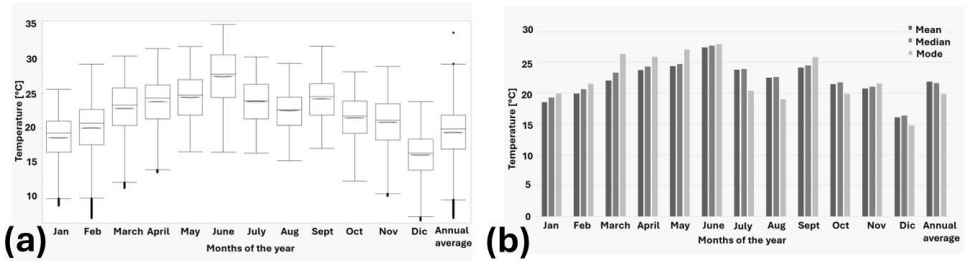

Figure 2: a) Box and whisker plots for ambient temperature during the year 2023. The horizontal line placed as a 'double line' in each of the boxes represents the mean of the data, b) biases of monthly and annual ambient temperature data.

Table 2: Measures of central tendency and interquartile range for ambient temperature [°C], relative humidity [%], wind velocity [m/s], and irradiance [W/m^2].

		Jan.	Feb.	March	Apr.	May	June	July	Aug.	Sep.	Oct.	Nov.	Dec.
Ambient	Mean	18.5	20.0	22.0	23.8	24.4	27.4	23.8	22.5	24.2	21.4	20.8	16.1
temperature	$Q2$	19.3	20.7	23.3	24.3	24.8	27.8	23.9	22.6	24.5	21.8	21.1	16.3
	$Q3-Q1$	4.4	5.2	5.4	4.9	5.1	6.1	5.0	4.1	4.6	4.7	5.2	4.5
Relative	Mean	35.5	34.3	26.8	25.6	32.0	27.4	47.4	54.0	42.0	51.0	44.7	56.6
humidity	$Q2$	32.5	33.0	23.9	22.0	28.0	24.0	46.0	53.8	40.2	51.8	45.0	57.0
	$Q3-Q1$	18.8	14.9	13.6	16.6	22.7	22.8	23.0	18.0	22.2	25.0	29.0	26.8
Wind	Mean	2.6	2.7	3.0	3.2	2.9	2.6	2.2	2.0	2.0	2.2	2.2	2.0
velocity	$Q2$	2.5	2.6	3.0	3.1	2.8	2.4	2.0	1.9	1.9	2.0	2.0	1.8
	$Q3-Q1$	1.8	1.7	2.0	1.9	1.9	1.5	1.2	1.2	1.2	1.2	1.3	1.4
Irradiance	Mean	519.6	586.6	683.7	728.6	656.0	720.1	638.8	579.0	641.2	474.4	470.8	347.0
	$Q2$	549.6	624.3	742.3	785.2	685.6	766.8	631.2	529.9	663.9	423.1	466.5	271.2
	$Q3-Q1$	469.5	213.2	496.6	521.1	589.4	514.7	634.9	641.7	582.9	542.1	525.2	455.2

The duos July and September, as well as October and November, overlap in most of the box, although their medians do not match. August presents the least variability in 50 % of the data (IQR = 4.10). July median (23.9 °C) and mean (23.8 °C) present very close values, the same effect occurs in the August box (mean 22.5 °C, median 22.6 °C). The distribution of the data is almost homogeneous in July and August, this implies that each of these months the data show symmetry. December has the lowest temperatures, 13.9 and 18.4 °C (Q1 and Q3), the temperature variation of 50 % of the data is 4.5 °C, and the average minimum and maximum temperature values are 7.2 and 23.8 °C. Between November and December there is no overlap of the boxes. Annually, 50 % of temperature data inside the boxes is concentrated between 19.0 and 25.0 °C, that is, an annual temperature variation of 5.8 °C. The annual maximum and minimum temperatures are 33.4 and 10.3 °C. In Figure 2b it can be seen that first six months, as well as in September and November, there is a negative asymmetric bias (mean<median<mode), so the lower half of the box is longer than the upper half. This means there is greater dispersion of the data. In July, August, October and December there is a positive asymmetric bias (mean>median>mode), that is, there is greater dispersion of data in the upper half of the box.

The same statistical analyzes were performed for the remaining environmental variables. Figure 3 shows the Box-plot diagrams that describe the annual behavior of relative humidity (3a), wind velocity (3b) and irradiance (3c). The relative humidity data present a positive asymmetry in general. This means that the 25 % of the data

contained in the upper part of the box is more dispersed, while the remaining 25 % tends to lower levels. The first six months of the year, 50 % of the data was in low to medium relative humidity ranges (15.0 to 42.7 %). The remaining half of the year presents an average increase of 47.4 % compared to March and April, the months with the lowest levels of relative humidity (18.0 to 33.0 %). As the year passes, the remaining months show an increase in relative humidity. However, the difference between the mean and the median decreases. Starting in May, the length of the boxes and whiskers increases, indicating an increasing variability of the relative humidity data. The number of outliers throughout the year does not exceed 1.27 %.
Data of wind velocity presents a positive asymmetry except for January and February the outliers represent only 1.29 %. The first six months of the year present greater dispersion of the data and 50 % of the data inside the box are between 1.7 and 4.1 m/s. The average of these six months ranges between 2.5 and 3.1 m/s. The annual wind velocity range where 50 % of the box data is concentrated is between 1.6 and 3.2 m/s, this represents an annual variation of 1.6 m/s. The remaining months speeds range between 1.2 and 2.8 m/s (30 % of reduction). It is worth noting that the months of January, February and June the boxes practically overlap; The same thing happens from March to May; in August, September and December; as well as in July, October and November. This means that there are at least two consecutive months, four times a year, that there are constant ranges of wind speed.

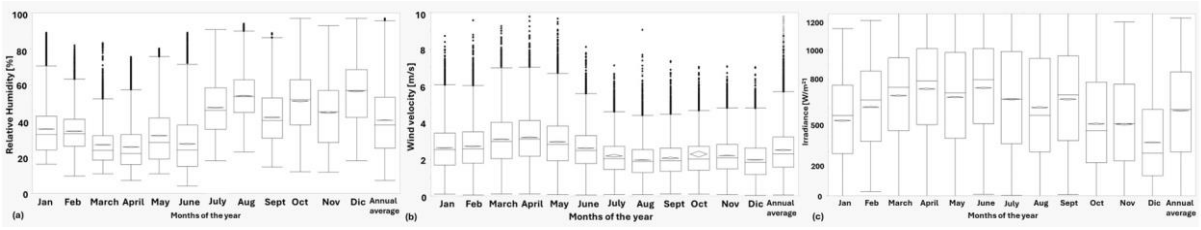

Figure 3: Box and whisker plots for (a) relative humidity, (b) wind velocity, and (c) irradiance during the year 2023.

The irradiance values are those that present the greatest dispersion of the four environmental variables studied, which is observed in such large interquartile ranges, with the highest being in the month of August, 641.70 W/m^2. The irradiance levels that can be reached during the day range from 0 (cloudy day) to 1,225 W/m^2. April and June presented the highest irradiance levels, where 50 % of their data range from 498.2 to 1,006.0 W/m^2 and with medians of 785 and 766 W/m^2 respectively. The minimum differences between the measures of central tendency (mean and median) correspond to the months of November and July with values of 4.3 and 7.64 W/m^2, also observing in these months that the boxes show a homogeneous distribution of the data and symmetry. The lowest levels of irradiance occur in December (128.2 to 559.0 W/m^2).

3.2 Drying kinetics

Solar dehydration of apple was carried out at a controlled temperature of 45 °C throughout the year. Figure 4 shows the drying curve, referring to the loss of average moisture content in three apple samples (A, B, C) with respect to time.

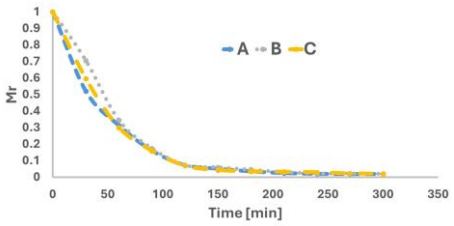

Figure 4: Moisture removal rate with respect to time of three apple samples (A, B and C) on April 21, 2023.

A test was carried out on April 21, 2023. On this day, maximum, minimum and average ambient temperature data were recorded (31, 20.8, and 26.5 °C), relative humidity (31, 11, and 18.3 %) and irradiance (1,139, 69.2, and 780 W/m^2). These conditions benefited the drying since this test had the shortest recorded time of 5 h (9:15 to 14:15 h), reducing the moisture content from 86 to 5 % on a wet basis, which represents a drying rate of 0.85

kg evaporated water/h. Since relative humidity was the environmental variable that increased up to 40 % in the middle of the year (July and August), drying kinetics was compromised and was reflected in drying times that increased by up to 40 %. That is, in the first half of the year, the average drying time was 5 h, while in the second half of the year, times of up to 7.2 h were recorded. The annual drying time is 6.4 h. The behavior of the ambient temperature and irradiance also had a significant effect on the process since the use of more energy was required to raise the temperature of the drying air. On the other hand, the diffusion coefficient experimentally determined was $1.93x10^{-10}$ m^2/s. This value is within the range published by a variety of authors, such as Elgamal et al. (2021) and Aktas et al. (2009) reporting values between $1.03x10^{-8}$ to $2.69x10^{-10}$ using forced convection solar devices with temperature ranges from 30 to 80 °C.

4. Conclusions

Knowledge of the behavior of the environmental variables helps to make predictions of drying times over a period, this is essential to design, construct and operate a solar dehydrator to guarantee the dehydration of fruits throughout the year in a city. Controlling the operating temperature of the dehydrator is essential to maintain the organoleptic properties and nutritional value of foods. The automation of the device that operates throughout the year at constant temperature of 45 °C and guarantees the dehydration of the apple, is a future improvement for temperature control. The operating temperature is a function of irradiance, relative humidity, wind speed and ambient temperature. In Guanajuato city, in general, ambient temperature and relative humidity are inversely related. April had the shortest drying times of up to 5 h, even when the highest levels of wind speed were recorded (6.65 m/s). Wind speed, ambient temperature and irradiance, are directly related to each other, and inversely related to relative humidity, with a significant impact on the drying kinetics, increasing drying times by 40 % for critical months such as December. Knowing the drying kinetics allows to maximize fruit production and the use of solar thermal energy, minimize the absorber area and reduce heat losses to the environment.

References

Aktas M., Ceylan I., Yilmaz S., 2009, Determination of drying characteristics of apples in a heat pump and solar dryer, Desalination, 239, 266–275.

Aviara N.A., Onuoha I.N., Faslola O.E., Igbeka J.C., 2014, Energy and exergy analyses of native cassava starch drying in a tray dryer, Energy, 73, 809-817.

Barros-Silva M., 2022, Evaluation of a solar dryer in different climatic and meteorological conditions, Research, Society and Development, 11(1), e15411124405.

Benseddik A., Azzi A., Chellali F., Khanniche R., Allaf K., 2018, An analysis of meteorological parameters influencing solar drying systems in Algeria using the isopleth chart technique, Renewable Energy, 122, 173-183.

Chaatouf D., Salhi M., Raillani B., Bria A., Amraqui S., Mezrhab A., 2023, Solar dryer analysis and effectiveness under four seasons with sensible and latent heat storage units, Innovative Food Science and Emerging Technologies, 85, 103310.

Crank J., 1975, The mathematics of diffusion. In: J.W. Arrowsmith Ltd., Clarendon Press, Oxford, UK, 76 – 88.

Duffie J.A., Beckman W.A., 2013, Solar Engineering of Thermal Processes, John Wiley & Sons, Inc. Hoboken, New Jersey, USA, 663-666.

ElGamal R., Kishk S., Al-Rejaie S., ElMasry G., 2021, Incorporation of a solar tracking system for enhancing the performance of solar air heaters in drying apple slices, Renewable Energy, 167, 676–684.

Gutiérrez-Pulido H., De-la-Vara-Salazar R., 2013, Quality basics. Chapter in: Statistical quality control and six sigma (Spanish), McGraw Hill Education, Mexico, 29-32.

Jowitt R., Escher F., Hallstrom B., Meffert H.F.Th., Spiess W.E.L.,Vos G.,(eds.), 1983, Physical Properties of Foods, Applied Science Publ.

Jowitt R., Escher F., Kent M., McKenna B., Roques M. (eds.). 1987, Physical Properties of Foods - 2. Elsevier.

Kamarulzaman A., Hasanuzzaman M., Rahim N.A., 2021. Global advancement of solar dryer technologies and its future prospect: A review, Solar Energy, 221, 559-582.

Majdi H., Esfahani J. A., 2019, Energy and drying time optimization of convective drying: Taguchi and LBM methods, Drying Technology, 37(6), 722–734.

Nukulwar M.R., Tungikar V.B., 2020, A review on performance evaluation of solar dryer and its material for drying agricultural products, Materials Today: Proceedings, 46, 345-349.

Rani P., Tripathy P.P., 2021, Drying characteristics, energetic and exergetic investigation during mixed-mode solar drying of pineapple slices at varied air mass flow rates, Renewable Energy, 167, 508–519.

Scheff S.W., 2016, Graphing Data. Chapter in: S. W. Scheff (Ed.), Fundamental Statistical Principles for the Neurobiologist, Academic Press, London, UK, 72-75.